

Performance improvement techniques for the DVB-RCS2 return link air interface

P. T. Mathiopoulos^{1,5,*}, E. A. Candreva², A. B. Awoseyila³, V. Dalakas^{4,5}, D. Tarchi²,
B. G. Evans³, A. Vanelli-Coralli² and G. E. Corazza²

¹*Department of Informatics and Telecommunications, National and Kapodistrian University of Athens, Athens, Greece*

²*Department of Electrical, Electronic and Information Engineering, University of Bologna, Bologna, Italy*

³*Institute for Communication Systems, University of Surrey, Guildford, UK*

⁴*Department of Informatics and Telematics, Harokopio University of Athens, Kallithea, Greece*

⁵*Institute for Astronomy, Astrophysics, Space Applications and Remote Sensing, National Observatory of Athens, Penteli, Greece*

SUMMARY

This paper presents performance improvement techniques for the second-generation digital video broadcast return channel via satellite air interface, which can be used for supporting future demands for Tbit/s traffic requirements. In particular, we have investigated minimum-shift keying (MSK) type of continuous phase modulation (CPM) waveforms by considering both single-carrier and multi-carrier transmission and single-amplitude and multi-amplitude signals, which improve the spectral efficiency. In addition, we consider frame timing and synchronization techniques, which make synchronization more accurate and robust. Our research has shown that the MSK single-carrier frequency-division multiple access (SC-FDMA) outperforms the quadrature phase-shift keying SC-FDMA in terms of resilience to distortion with the performance gap increasing when the amplifier shows a milder distortion. The performance of a multi-amplitude CPM scheme, based upon the superposition of two single-amplitude MSK signals at the radio frequencies level, is also investigated. In comparison with other equivalent linear modulation schemes, performance evaluation results have been shown that the proposed multi-amplitude CPM scheme significantly improves the spectral efficiency in the presence of adjacent channel interference. Finally, we have proposed a viable and efficient methodology, which enables reliable and accurate timing and frequency synchronization for the SC-FDMA satellite return link. This involves a combination of global positioning system (GPS)-based pre-compensation of differential timing between user terminals, preamble detection in an integrated random access channel, and user channel frequency estimation based on repetitive symbols in the time domain. Copyright © 2015 John Wiley & Sons, Ltd.

Received 14 November 2014; Revised 30 April 2015; Accepted 16 June 2015

KEY WORDS: SC-FDMA; CPM; multi-amplitude CPM; MSK; return link; frame timing; synchronization; DVB-RCS2

1. INTRODUCTION

The ever-increasing commercial demand for higher user data rates via satellites has led to the adoption of the second-generation digital video broadcast return channel via satellite (DVB-RCS2) system [1]. This standard, designed by the digital video broadcasting (DVB) project, defines the complete air interface specification for two-way satellite broadband very small aperture terminals. The first-generation digital video broadcast – return channel via satellite (DVB-RCS) standard was published as EN 301 790 [2], while the substantially more powerful DVB-RCS2 was published in three parts as TS 301 545-1 Overview and System Specification, (OSL) [3], EN 301 545-2 Lower Layer for Satellite, (LLS) [4], and TS 301 545-3 Higher Layer for Satellite, (HLS) [5]. Although the DVB-RCS2 defines

*Correspondence to: P. T. Mathiopoulos, Department of Informatics and Telecommunications, National and Kapodistrian University of Athens, Panepistimioupolis, Ilisia, Athens 157 84, Greece.

†E-mail: mathio@space.noa.gr

the transmissions parameters, it leaves open to the designer the adoption of specific receiving communication techniques. This allows the design of the most appropriate receivers, which should achieve the necessary performance depending upon required services.

The research reported here focuses on the issue of increased traffic demands for the future Internet in the '2020 and Beyond' time frame, such as the requirement for Tbit/s traffic [6]. Towards this end, the European Satellite Agency (ESA), through its Advanced Research in Telecommunications Systems 1 program, has identified several key issues, which limit the desired Tbit/s satellite capabilities [7]. In this paper, an effort is made to investigate techniques, which aim at improving the spectral efficiency (SE), performance, and cost effectiveness of the air interface as well as dealing with the limitations imposed by interference. The proposed enhancements are expected to support the satellite broadband networks evolution towards an ultra-high capacity satellite communications system. In particular and within the framework of the DVB-RCS2 standard, the following research topics will be investigated:

- (1) Continuous phase modulation (CPM) waveform design by considering single-carrier and multi-carrier transmission as well as single-amplitude and multi-amplitude signals.
- (2) Frame timing and carrier frequency synchronization for multi-carrier transmission.

Regarding the first topic, for the last three decades or so, the subject of CPM, which typically is single amplitude with constant envelope signals, has been investigated quite extensively in connection with the design of various transmitter/receiver (transceiver) structures (e.g., see [8] and the references therein). Thanks to their compact spectrum properties, especially in the presence of non-linear distortion, CPM signals have been used in various telecommunication standards [9]. In satellite communications, for instance, in addition to linear modulation (LM) signals, various CPM signals have been adopted in the DVB-RCS2 standard [1].

The lesson learnt from the DVB-RCS2 standardization procedure is that, in general, CPM and LM have comparable performance for low-to-medium SE [10]. For example, for SE up to 1.5 bit/s/Hz, CPM and LM schemes perform similarly for a given signal-to-noise ratio reference value. However, for this SE range, CPM appears to be more cost efficient than LM, mainly because of the more relaxed requirements imposed on the radio frequencies (RF) front end of the terminal [10]. On the other hand, LM appears to be a more appropriate solution for higher SE, because it allows to reach higher SE values with respect to the equivalent CPM schemes [11]. In our current research and in order to increase the SE of CPM signals, the performance of multi-amplitude CPM (MA-CPM) signals [12] is investigated for the first time in the context of satellite communication systems. Independently from the employed modulation scheme, a widely known trend in terrestrial communication systems is to move from single-carrier to multi-carrier schemes, because the latter are particularly resilient to the impairments typically encountered in a terrestrial radio link [13, 14]. Their resistance to non-linear distortion and flexibility in resource allocation are the reasons that multi-carrier transmission was first adopted in wired systems [15] and subsequently to wireless telecommunication systems, for both broadcast and point-to-point communications [14, 16]. It is noted that their extensive use in wireless terrestrial communications and their characteristics in terms of resistance to non-linear distortion and flexibility in resource allocation have pushed toward their adoption in satellite communications, allowing also a higher compatibility between terrestrial and satellite waveforms, thus increasing their possible cooperation.

Motivated by the foregoing discussion, on the first topic considered in this paper, we propose and evaluate the performance of new single-amplitude and MA-CPM waveforms, in connection with the multi-carrier systems by mainly targeting improvements in SE. Similar to [17], we consider CPM signals with modulation index $h = 1/2$ because of their implementation simplicity and their relative compact spectrum, as well as their relatively simple receiver structures. Although such waveforms are usually referred to as minimum-shift keying (MSK)-type CPM signals, for the convenience of the presentation, from now the terms 'CPM' and 'MSK' will be denoting the same 'MSK-type' of signals.

The first part of the CPM signal study is devoted toward the analysis and optimization of the mapping schemes to be used in a multi-carrier satellite environment. To this aim, a fair comparison between LM and CPM schemes will be considered, by taking into account the non-linear effects introduced by the high power amplifier (HPA). In particular by employing different HPA models, we study their effects on the in-band distortion, in terms of modulation error ratio (MER) and out-of-band spectral regrowth.

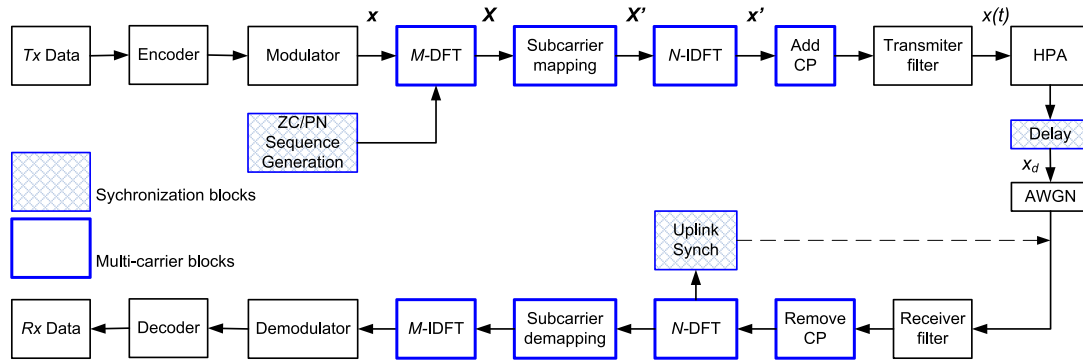


Figure 1. Block diagram of the system model. CP, cyclic prefix; DFT, discrete Fourier transform; HPA, high power amplifier; IDFT, inverse discrete Fourier transform; PN, pseudo-random noise; ZC, Zadoff–Chu.

Among several possible CPM schemes, we resorted to an MSK-type CPM signal, which avoids the zero cross in the signal waveform, a condition that is detrimental when HPA is employed. In the context of a single-carrier frequency-division multiple access (SC-FDMA) scenario, we investigate and analyze the performance of various single-amplitude CPM signals. Furthermore, we consider a MA-CPM signal in the same access scenario but with single user detection. For the latter case, the selection of the waveforms is such that the proposed MA-CPM signals essentially double the SE achieved by the single-amplitude CPM signals proposed in the DVB-RCS2 standard at the expense of an increased power requirement.

On the second topic of our research, we study frame timing and carrier frequency synchronization within the context of a future DVB-RCS2 signal based on an SC-FDMA waveform, as specified in [1]. In this regard, it should be noted that the SC-FDMA waveform acts as a carrier for modulated symbols, which have been pre-processed and mapped to different sub-carriers (see Figure 1 and Section 2 for details). It is well known that multi-carrier communications have strict requirements in terms of synchronization due to their exploitation of multiple narrower bands [18]. Moreover, the satellite environment poses additional challenges in terms of synchronization [19, 20]. Therefore, we have investigated SC-FDMA synchronization in the geostationary Earth orbit (GEO) satellite fixed channel. The proposed solution involves frame timing pre-compensation, preamble detection in an integrated random access channel (RACH), appropriate cyclic prefix (CP) dimensioning, and user channel frequency estimation.

The organization of the paper is as follows. After this Introduction, in Section 2, the generic and detailed system model that was used in our study is presented. Section 3 proposes efficient mapping schemes for single-amplitude CPM signal in SC-FDMA systems. Section 4 presents MA-CPM transceiver structures as well as performance evaluation results, including SE improvements. Section 5 deals with frame timing and carrier frequency synchronization issues within an SC-FDMA system including synchronization acquisition using the RACH at logon and synchronization tracking using training sequences in the shared user data channel. Conclusions can be found in Section 6.

2. SYSTEM MODEL

The block diagram of the system model under consideration, shown in Figure 1, represents the equivalent baseband of the uplink of a typical multi-user satellite communication system.

A user may transmit independent CPM signals, single-amplitude or multi-amplitude and/or single-carrier or multi-carrier. These signals are passed through a non-linear HPA and then transmitted through the channel. Corrupted by additive white Gaussian noise (AWGN) with single-sided power spectral density, N_0 , the signals arrive at the satellite, in the general case, asynchronously. Because we have considered CPM waveform design for single-carrier and multi-carrier transmissions, the blocks of Figure 1 employed for multi-carrier transmission are depicted with bold borders. In the same figure, the blocks used for implementing asynchronous reception, which are not considered in case of synchronous reception, are marked with shades. Because the multiple access scheme used for downlink

differs from the one used for the uplink [21], the system model under consideration assumes that with perfect timing synchronization, the user signals are demultiplexed and fully recovered at the satellite from the aggregated signal.

The first blocks of Figure 1 encode and modulate the information bits to be sent. The modulator is a key part of this study, where alternatively LM or CPM is employed. After the modulator, a discrete Fourier transform (DFT) block, depicted as M -DFT, where M is the order of the transformation, processes the signal prior to the sub-carriers allocation. The DFT is the key for the beneficial properties of the SC-FDMA envelope, which has properties closer to that of a single-carrier signal rather than that of an orthogonal frequency-division multiple access (OFDMA) signal, hence allowing a higher resilience to non-linear distortion. After the DFT, the sub-carrier mapping block allocates the output of the DFT to the sub-carriers of the SC-FDMA symbol. The following two mappings strategies are considered:

- Localized carrier frequency-division multiple access (LFDMA) whereby each user is assigned a contiguous group of sub-carriers.
- Interleaved frequency-division multiple access (IFDMA) whereby each user's sub-carriers are evenly interlaced with the other users sub-carriers.

After the sub-carrier allocation, an inverse discrete Fourier transform (IDFT) operation is employed before the CP insertion.

If we consider the return link of a satellite communication system where each user emits M symbols $x_k, k = 1, 2, \dots, M$, obtained through a proper mapping of coded information bits, the vector, \mathbf{x} , which groups the symbols x_k , is processed via a DFT to obtain the vector \mathbf{X} as follows:

$$\mathbf{X} = \mathbf{F}_M \mathbf{x} \quad (1)$$

where \mathbf{F}_M is the DFT matrix having order M . In case of LFDMA, \mathbf{X} is zero padded with $N - M$ zeros, to form \mathbf{X}' , while in case of IFDMA, \mathbf{X} is up-sampled by a factor N/M , to obtain the vector \mathbf{X}' still having length equal to N . Mathematically, this can be expressed as follows:

$$\mathbf{X}' = [\underbrace{X_1, X_2, \dots, X_M}_M \underbrace{00 \dots 0}_{N-M}] \quad (2)$$

in case of LFDMA, and

$$\mathbf{X}' = [X_1, \underbrace{0 \dots 0}_{\frac{N-M}{M}}, X_2, \underbrace{0 \dots 0}_{\frac{N-M}{M}} \dots X_M \underbrace{0 \dots 0}_{\frac{N-M}{M}}] \quad (3)$$

in case of IFDMA. Vector \mathbf{X}' , corresponding to either LFDMA or IFDMA, is further processed through an IDFT, thus obtaining the vector $\mathbf{x}' = \mathbf{F}_N^* \mathbf{X}'$. Then a CP is inserted, and the signal through the transmit filter is converted to analog, yielding $x(t)$, frequency up-converted, amplified, and transmitted.

The SC-FDMA can yield the advantages of a commonality with terrestrial waveforms while providing an acceptable resilience to non-linear distortion. There are two degrees of freedom, which can be exploited to improve such resilience. On the one hand, the sub-carrier allocation, that is, LFDMA or IFDMA, can be efficient in reducing the intermodulation effects. On the other hand, the user's symbol set can provide an additional margin against distortion. For example, although it is known that a quadrature phase-shift keying (QPSK) modulation is very robust to channel impairments and transceiver non-linear behavior, it is still unclear whether or not this is the best possible mapping in terms of resilience to non-linear distortion for SC-FDMA. For this reason, in the following, we consider two possible modulations for the x_k symbols: (i) a conventional QPSK modulation, in which the symbols are drawn from the alphabet

$$\mathcal{X}_{QPSK} = \left\{ \frac{1+J}{\sqrt{2}}, \frac{1-J}{\sqrt{2}}, \frac{-1+J}{\sqrt{2}}, \frac{-1-J}{\sqrt{2}} \right\} \quad (4)$$

and (ii) an alternate modulation scheme based on MSK signals, in which we use the signal set as shown previously but avoid a π phase-shift signal transition among consecutive symbols, thus allowing only $\pi/2$ phase transitions. Mathematically, a time-continuous baseband MSK signal can be expressed as follows:

$$m(t) = \sum_{k=0} (1 - 2b_{2k}) \cos\left(\frac{\pi t}{2T_b}\right) - (1 - 2b_{2k+1}) \sin\left(\frac{\pi t}{2T_b}\right) \quad (5)$$

where b_k are the information bits, $1 - 2b_k$ is the mapping from bits to antipodal symbols, and T_b is the bit duration.

For the proposed SC-FDMA mapping, the aforementioned signals are sampled at a rate equal to the bit time, and we obtain samples that belong to a QPSK constellation while avoiding a π phase shift between two consecutive symbols. Notably, a difference with respect to [22] is that we neglect trellis termination, so this mapping yields the same SE of a QPSK modulation.

The analog signal $x(t)$ is then amplified by an HPA having non-linear characteristics when it operates near to its saturation point. In general, the amplifier output can be expressed as follows:

$$x_d(t) = G[\rho(t)]e^{J\{\psi(t)+\Phi[\rho(t)]\}} \quad (6)$$

where $\rho(t)$ and $\psi(t)$ represent the envelope and the phase of $x(t)$, and $G[\cdot]$ and $\Phi[\cdot]$ represent the AM/AM and AM/PM characteristics of the HPA, respectively.

In the following, we present three commonly used models for various non-linear HPA. Note that we consider only memoryless, frequency-flat HPA models, in which the current output signal depends only on the input current signal, and the characteristics of the HPA do not depend on the frequency of the input signal.

A solid-state HPA is commonly modeled using the Rapp [23] AM/AM transfer function, that is,

$$G[\rho] = \frac{\rho}{2^p \sqrt{1 + \rho^{2p}}} \quad (7)$$

where p is a parameter of the model known as smoothing factor, which typically takes a value equal to 2.

Because an HPA can also have a phase conversion effect, which is not present in the Rapp model, for this model, the AM/PM curve was mimicked with a parabolic transfer function. Such HPAs, with strong phase conversion characteristics, are commonly modeled according to Saleh's model [24], where the non-linear gain function $G[\rho]$ and the non-linear phase function $\Phi[\rho]$ are commonly expressed as follows:

$$G[\rho] = \frac{\alpha_a \rho}{1 + \beta_a \rho^2} \quad (8)$$

$$\Phi[\rho] = \frac{\alpha_p \rho^2}{1 + \beta_p \rho^2} \quad (9)$$

with parameters α_a , β_a , α_p , and β_p assuming typical values taken from [24].

For the third amplifier model, we considered the so-called clipping amplifier [25]. In particular, assuming that the amplifier is ideally predistorted, its characteristics will be, up to a certain value, linear and then flat, because the predistorter would be unable to efficiently compensate the amplifier distortion after a certain level. In this case, the ideal clipping model is used to the cascade of predistorter and amplifier, so that

$$G[\rho] = \min\{\rho, 1\} \quad (10)$$

3. EFFICIENT MAPPING SCHEMES FOR SINGLE-CARRIER FREQUENCY-DIVISION MULTIPLE ACCESS

This section proposes an efficient mapping scheme suitable for SC-FDMA satellite communications. As previously mentioned (Section 2), we focus on two possible mapping schemes belonging to the LM and CPM families, respectively.

The adaptation of waveforms, which are typically used in single-carrier satellite communication systems, to equivalent ones employing multi-carrier systems, is not straightforward as their interchangeable use does not necessarily lead to improved performance. For example, the currently used waveforms for single-carrier satellite communication systems are selected for certain fading channel models [26]. These waveforms are not necessarily the most appropriate for multi-carrier systems mainly due to the intrinsic characteristics of multi-carrier communications, especially in terms of high peak-to-average power ratio (PAPR), leading to detrimental effects to the satellite transceiver [27].

Moreover, the waveforms designed for single-carrier communications cannot exploit the advantages of multi-carrier communications due to their higher sensitivity in the presence of non-linear distortion, which is typical of a satellite communication system [28]. Naturally, the possibility of having a similar and compatible waveform between satellite and terrestrial systems has been considered in the past, as an important advantage for enhancing the interoperability between these two communications systems [29]. To this end, it is noted first that there are several examples of multi-carrier modulations for satellite systems, for example, considering the normative documents, we can cite the digital video broadcast – next-generation handhelds [30] and the DVB-RCS2 implementation guidelines [31].

For these cases, the waveform is based on SC-FDMA, which preserves the advantages of multi-carrier schemes, but has smaller envelope fluctuation as compared with OFDMA, thus being more suitable for the non-linear satellite channel [27]. The use of single-amplitude CPM signals in connection with SC-FDMA was first proposed in [22]. In particular, it was shown that it is possible to achieve a quasi-constant envelope for an SC-FDMA waveform by employing single-amplitude CPM signals, with increased robustness to non-linear distortion. Further, the adoption of a modulation scheme with memory allows the use of iterative demodulation-decoding algorithms, with an improvement in the detection performance.

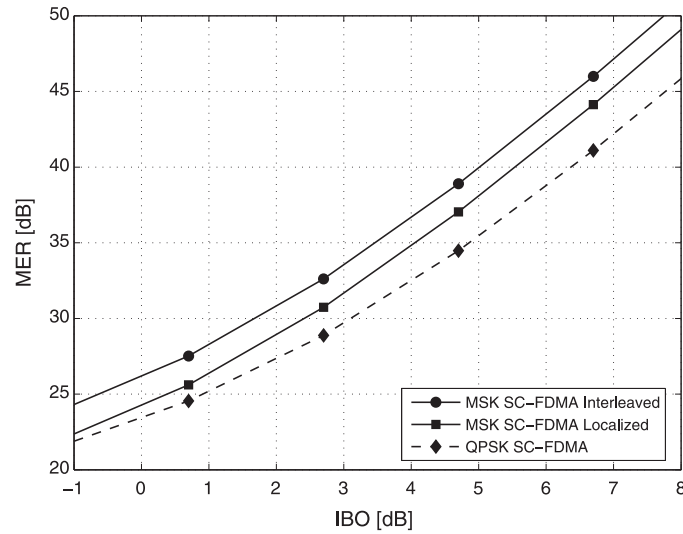
To design an SC-FDMA waveform suitable for satellite communications, and hence resilient to non-linear distortion, a possible solution is presented here by using CPM signals. For this task, we are targeting cost efficiency as well as SE. Note that the potential cost improvement can be achieved with either an increase of the SE or a reduction in the terminal cost, the latter being significantly influenced by the cost of the RF component rather than the baseband component. For this reason, our attention is focused on waveforms, which are robust to non-linear distortion, so that they can be employed in conjunction with low-cost HPA. Building upon [17], we focus on the simplest case of CPM, that is, MSK, and we present results for the in-band distortion and out-of-band spectral regrowth of an SC-FDMA system based on MSK modulation [32]. Intuitively, the cascade of DFT and IDFT blocks of an SC-FDMA transmitter can still preserve some of the features of the signal, so that in case the mapping symbols have slow phase transitions, the output will still have slow dynamics. In this way, it is expected that the output signal will be less affected by non-linear distortion.

In the following, we consider an SC-FDMA system with 1024 sub-carriers allocated to four users, either in a localized or in an interleaved fashion. The performance results have been derived considering the MER as the figure of merit, which gives a quantitative insight on the in-band distortion, and the signal spectrum as a qualitative insight on the out-of-band distortion. The MER is defined as the ratio between the average energy of the signal constellation and the energy of the error, which is the difference between the received symbol and the original constellation point [33]. In mathematical terms, letting \hat{x}_k , where $k = 1, 2, \dots, M$, be the received counterpart of x_k , we have

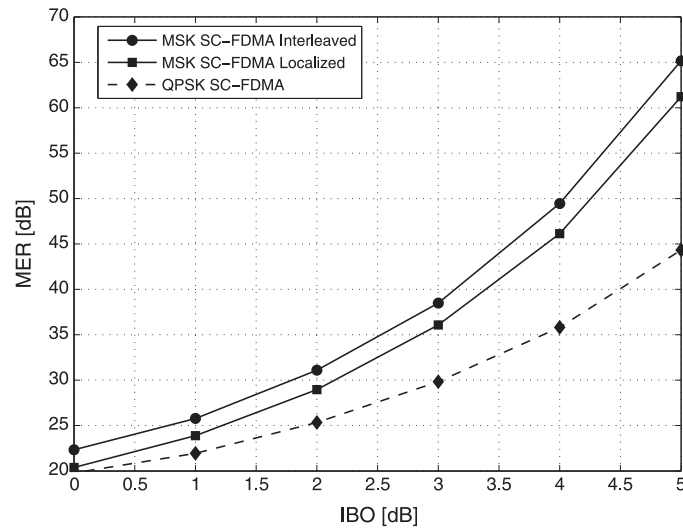
$$\text{MER} = \frac{\sum_{k=1}^M |x_k|^2}{\sum_{k=1}^M |\hat{x}_k - x_k|^2} \quad (11)$$

From the foregoing equation, it is clear that the MER can be seen as the inverse of the normalized mean square error. It is noted that this figure of merit is more accurate than the PAPR in predicting the system performance. This happens because a PAPR plot shows the tails of the signal amplitude distribution, hence providing a qualitative insight on the performance, while the MER quantitatively shows the impact of the signal dynamics after a non-linear amplification device.

First, we focus on the in-band distortion, showing in Figure 2 the performance in terms of MER for the two different amplifier models, that is, Rapp and ideal clipping for a variable input backoff (IBO). The comparison has been performed for interleaved and localized MSK and for QPSK with IFDMA.



(a) Rapp amplifier



(b) Ideal Clipping

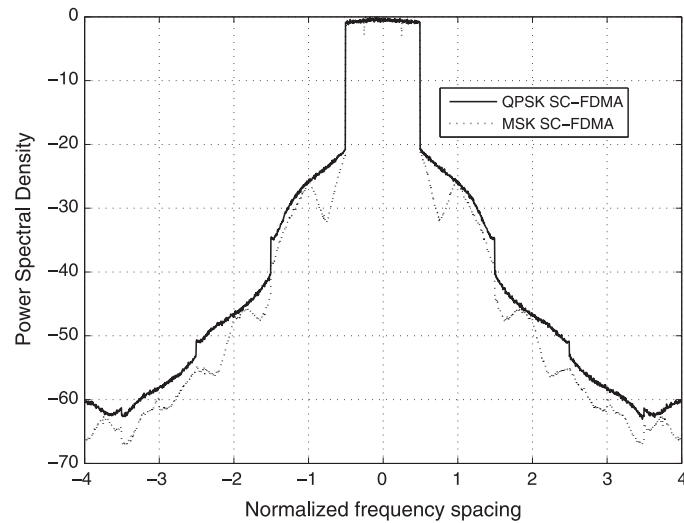
Figure 2. Modulation error ratio (MER) versus input backoff (IBO) for minimum-shift keying (MSK) single-carrier frequency-division multiple access (SC-FDMA) and comparison with quadrature phase-shift keying (QPSK) SC-FDMA: (a) Rapp amplifier and (b) ideal clipping.

The QPSK with IFDMA is used as a benchmark because it can be considered as the sub-carrier mapping scheme with the best performance over non-linear channels [27]. The IBO is an important system parameter describing the amplifier operating point by relating the saturation power of the HPA to the average power of the input signal, that is,

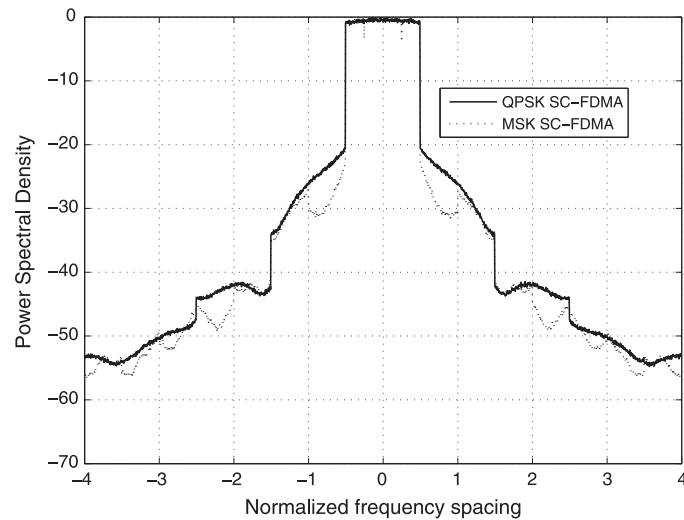
$$IBO \doteq \frac{P_{in}^{sat}}{P_{in}} \quad (12)$$

where P_{in}^{sat} is the input saturation power, $P_{in} = E[|x(t)|^2]$ is the average input power, and $E[\cdot]$ denotes the expectation operator.

As the performance evaluation results of Figure 2 illustrate, the interleaved SC-FDMA is more resilient than the localized SC-FDMA. This finding is consistent with the results presented in [27]. However, more interesting is the observation that the MSK mapping outperforms the QPSK mapping



(a) Rapp amplifier



(b) Ideal Clipping

Figure 3. Power spectral density of the QPSK SC-FDMA and the MSK SC-FDMA signals with $IBO = 0$ dB: (a) Rapp amplifier and (b) ideal clipping. IBO, input backoff; MSK, minimum-shift keying; SC-FDMA, single-carrier frequency-division multiple access; QPSK, quadrature phase-shift keying.

not only for a Rapp-modeled amplifier but also in case of an ideal clipping amplifier, which corresponds to the case of ideal predistortion. Furthermore, in order to investigate the out-of-band figures of merit, the spectra for interleaved MSK SC-FDMA and interleaved QPSK SC-FDMA after non-linear distortion have been obtained and are illustrated in Figure 3. From these results, it can be observed that the MSK SC-FDMA spectrum is always lower than the QPSK SC-FDMA spectrum, in the first adjacent bands when ideal clipping is considered and over all the adjacent bands in case of Rapp amplifier.

In summary, our results have been shown that the MSK SC-FDMA is always outperforming the QPSK SC-FDMA, and the performance gap increases when the amplifier shows a milder distortion.

4. MULTI-AMPLITUDE CONTINUOUS PHASE MODULATION SCHEMES

As mentioned in the Introduction, in order to increase the SE of CPM signals, a natural approach is to employ MA-CPM signals [12]. Here, we revisit the subject of MA-CPM because it has received

only limited attention in the past possibly because of their complex signal structure as well as the rapid advancement and accumulated know-how for quadrature amplitude modulation (QAM) type of LM signals. Thus, on this subject, there have been very few papers published in the open technical literature, for example, [12, 17, 34, 35]. In particular, the spectral and distance characteristics of MA-CPM signals have been investigated in a linear channel [34]. In [12], some very general transceiver structures for MA-CPM signal have been presented. In [35], the performance of MA-CPM signals has been evaluated for optical communication systems. In [17], a detailed performance study of MA-CPM signals based on MSK modulation formats, which have been termed as multi-amplitude MSK, has been presented. More specifically, this paper investigated the performance of a two-amplitude minimum-shift keying (2A-MSK) in the presence of an AWGN channel by including also the effect of non-ideal synchronization and various experimental performance evaluation results.

Following [17], we have investigated the performance of the transmitted structure illustrated in Figure 4. It consists of two MSK modulators, like the ones described from (5), followed by square root raised cosine (SRRC) filters with an excess bandwidth α and two non-linear HPAs.

In order to implement the desired 2A-MSK signal, the amplitude of the signal at the output of the second MSK modulator is multiplied by a factor of two. Unless otherwise stated, it is assumed that both MSK modulators and SRRC filters are identical, and the two HPAs follow the Rapp model as described in Section 2. The main advantage of this transmitter structure is that the two transmitted MSK signals, superimposed at RF, maintain their constant envelope properties, so that their out-of-band energy after the non-linear amplification remains low. On the other hand, the disadvantage of this approach is that it requires the use of an additional HPA. The proposed transmitter has been implemented in software, and typical state-space diagrams (with or without SRRC filtering) obtained by means of computer simulations are illustrated in Figure 5.

The block diagram of the receiver structure is depicted in Figure 6, where it is assumed that the receiver has perfect carrier and symbol timing synchronization. The decision logic block appropriately separates the two amplitude signals' levels to recover the initial transmitted information sequences.

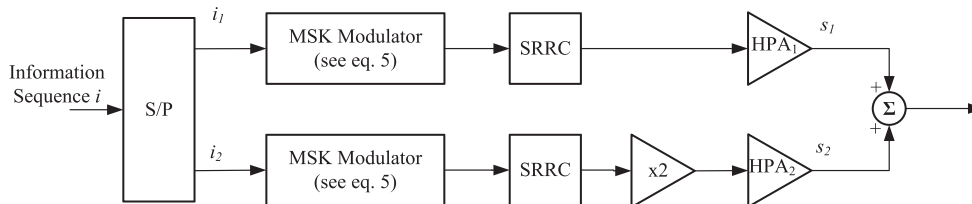


Figure 4. Block diagram of the two-amplitude MSK transmitter. HPA, high power amplifier; MSK, minimum-shift keying; SRRC, square root raised cosine.

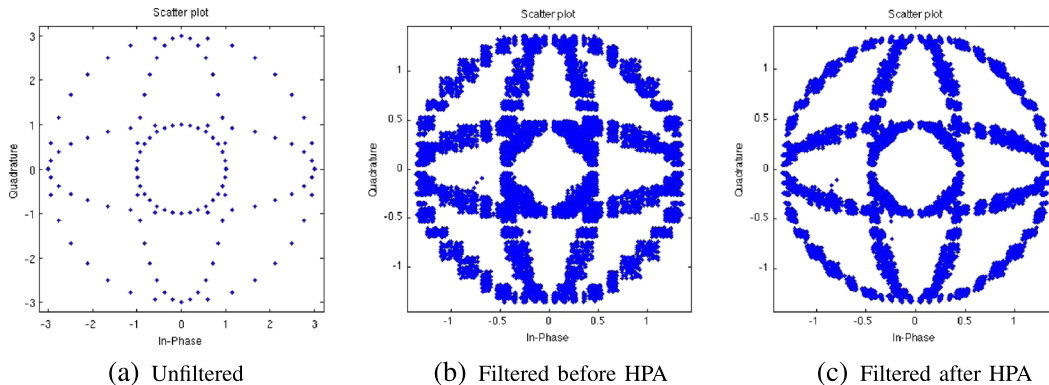


Figure 5. State-space diagrams of the transmitted two-amplitude minimum-shift keying signal: (a) unfiltered, (b) filtered before high power amplifier (HPA), and (c) filtered after HPA.

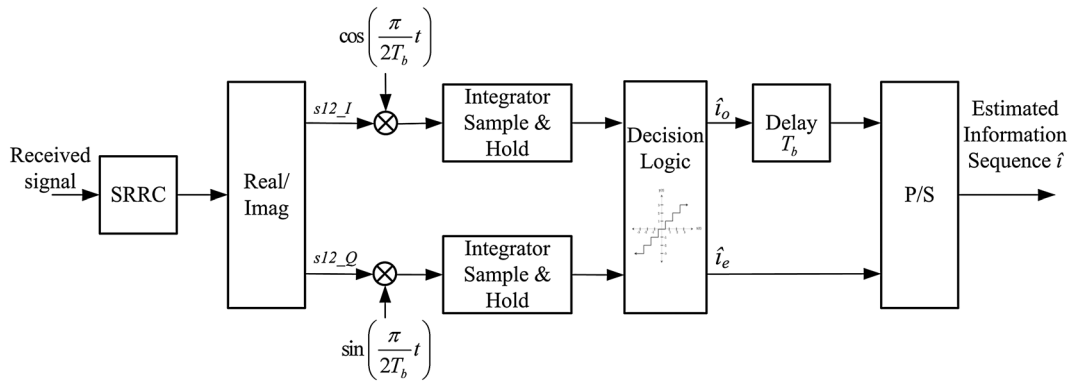


Figure 6. Block diagram of the two-amplitude minimum-shift keying receiver. SRRC, square root raised cosine.

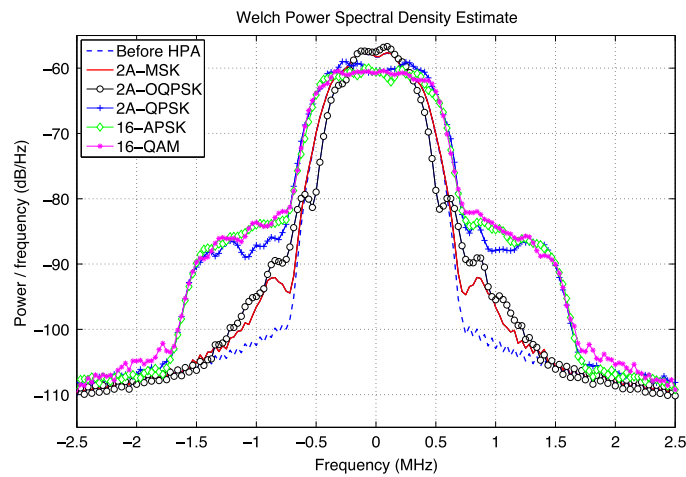


Figure 7. Power spectral densities of the transmitted multi-amplitude signals after the high power amplifier (HPA). APSK, amplitude and phase-shift keying; 2A-MSK, two-amplitude minimum-shift keying; QPSK, quadrature phase-shift keying; 2A-QPSK, two-amplitude QPSK; OQPSK, offset QPSK; 2A-OQPSK, two-amplitude OQPSK; QAM, quadrature amplitude modulation.

The performance of the proposed transceiver structure has been tested by a series of computer-simulated experiments, and various evaluation results have been obtained by means of Monte Carlo trials. For a fair comparison, we have also evaluated the performance of equivalent LM signals, that is, two-amplitude QPSK (2A-QPSK) and offset QPSK (OQPSK) signals, termed as 2A-QPSK and two-amplitude OQPSK, respectively. Their implementation is very similar to the 2A-MSK implementation, the only difference being the replacement of the two MSK modulators shown in Figure 4 and an equivalent modification of the receiver structure shown in Figure 6. The performance evaluation results were also compared with similar results obtained for the more traditional multi-amplitude schemes such as 16-QAM and 16-amplitude and phase-shift keying (16-APSK). Unless otherwise stated, all the results have been obtained with SRRC filters with $\alpha = 0.35$.

The first set of performance evaluation results showing the advantage of the transmitted 2A-MSK signal is presented in Figures 5 and 7. Its insensitivity to non-linear distortion can be clearly observed by comparing the state-space diagrams of Figure 5(b) and 5(c) (before and after non-linear amplification). This can be also noted from Figure 7 where the proposed 2A-MSK signal outperforms in out-of-band spectral regrowth, the equivalent (in terms of SE) 16-QAM and 16-APSK signals. The performance of these three modulation formats has been further evaluated, and detailed performance comparisons in terms of additional performance criteria, including bit error rate (BER) and total degradation (TD), have been obtained in [36]. However, because of space limitations, here, we will be focusing on their SE performance, and only a brief summary of our most important findings with

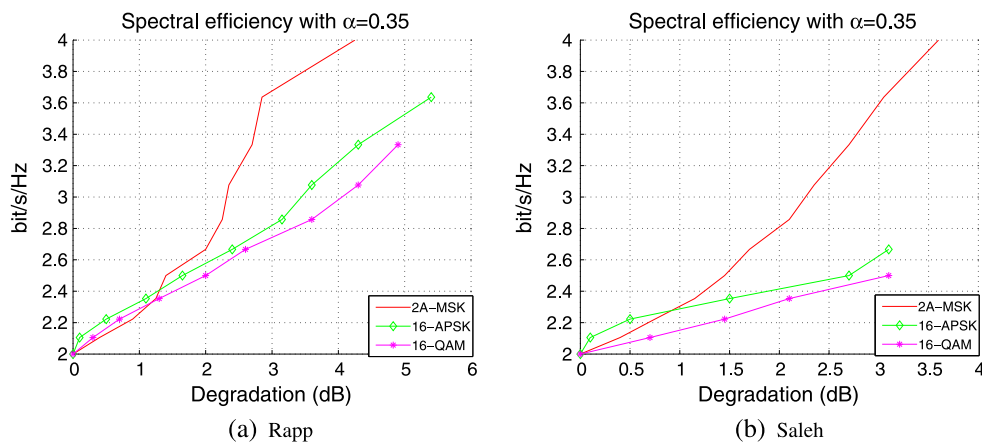


Figure 8. Spectral efficiency versus adjacent channel interference degradation for the proposed two-amplitude minimum-shift keying (2A-MSK) transceiver in the presence of a high power amplifier: (a) Rapp and (b) Saleh. APSK, amplitude and phase-shift keying; QAM, quadrature amplitude modulation.

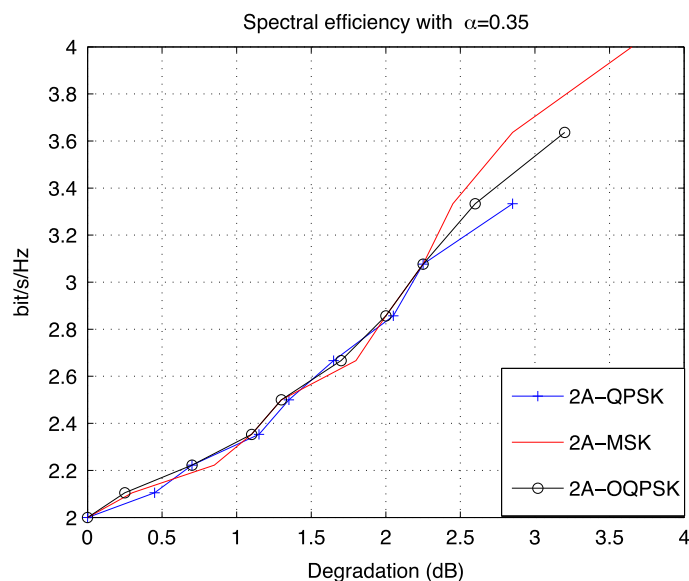


Figure 9. Spectral efficiency versus adjacent channel interference degradation for the proposed two-amplitude minimum-shift keying (2A-MSK) transceiver without a high power amplifier. QPSK, quadrature phase-shift keying; 2A-QPSK, two-amplitude QPSK; OQPSK, offset QPSK; 2A-OQPSK, two-amplitude OQPSK.

respect to the other performance criteria will be presented. The detailed overview of the complete set of results has been presented in [36]. For example, it was found that although the BER performance of these modulation schemes in an AWGN channel is similar, the TD performance of the proposed 2A-MSK was the best. We have also investigated the sensitivity of the 2A-MSK scheme in the presence of non-linear HPAs with different phase characteristics, that is, with AM/PM distortion using the Saleh model [24]. The obtained results have been shown that for a phase difference of 10° , there is a TD degradation of less than 2 dB, as compared with the case where the two HPAs are identical. In this case also, the proposed 2A-MSK significantly outperforms the other two modulation schemes. Moreover, BER performance evaluation results for a coded 2A-MSK modulation scheme have been obtained for a binary, non-systematic, and non-recursive convolutional code with a rate of $1/2$ and a polynomial trellis of (3 5 7), which has been proposed in the DVB-RCS2 standard. It is noted that the receiver structure shown in Figure 6 was slightly modified in order to include the appropriate hard decision decoding necessary for appropriate signal detection.

Focusing now on the SE performance, Figure 9 presents the SE versus degradation (for a BER level of 10^{-3}), which occurs because of an artificial increase of the adjacent channel interference (ACI). For obtaining the SE, we have used the approach suggested by the DVB-RCS2 standard [4, p. 177], that is,

$$SE = \frac{R_c \cdot \log_2(\Lambda)}{D_f \cdot T_s} \quad (13)$$

where R_c is the code rate, D_f the carrier spacing, Λ the constellation order, and T_s the symbol duration. In our simulations, although we used the same levels of ACI as those used to obtain the performance results reported in DVB-RCS2, we have used only two adjacent channel interferers (one above and below the useful signal), instead of the four adjacent channel interferers used in the DVB-RCS2 standard. As illustrated in Figure 8, the SE achieved by the proposed 2A-MSK modulation is almost 4 b/s/Hz, whereas the CPM modulation schemes used in the standard achieve only 1.8 b/s/Hz (with a convolutional code rate of 6/7) – see [4, Table 10.7, p. 178].

Finally, we have performed SE comparisons for the 2A-MSK and the 16-APSK and 16-QAM schemes assuming that the second amplifier depicted in Figure 4 is operating at 0-dB IBO, while the first one is operating at 6-dB IBO (due to the x^2 factor of the second signal component). As shown in Figure 8, in terms of SE, the proposed scheme can double the SE currently achieved by (single amplitude) CPM signals proposed in the DVB-RCS2 standard. It is noted that we have not included the other two hierarchical schemes as they have inferior SE performance (Figure 9). Figure 8(a) shows the achieved SE versus degradation, which occurs because of artificially increasing ACI in the case that we are operating at 0-dB IBO with amplifiers following the Rapp model. The obtained SE performance evaluation results clearly show the significant superiority of the proposed 2A-MSK scheme. Figure 8(b) illustrates the achieved SE versus degradation, which occurs because of amplifiers following the Saleh model for the same candidates (this model was considered to illustrate the possibility to have phase changes). Similarly to the Rapp model case, this plot shows again the significant SE performance gains that the 2A-MSK scheme can achieve in ACI environments compared with LM.

5. SINGLE-CARRIER FREQUENCY-DIVISION MULTIPLE ACCESS SYNCHRONIZATION

As well known, SC-FDMA is a multi-carrier air interface, which makes use of orthogonal sub-carriers, and orthogonality requires timing and frequency precision. In this section, we investigate SC-FDMA synchronization in the GEO satellite fixed channel using preamble-aided techniques and an integrated RACH. In this regard, our study is independent of the modulation scheme (e.g., QPSK or CPM) used for the data sub-carriers. We demonstrate how frame timing synchronization can be achieved for a new user entering the network and consider the effect of the GEO satellite drift on cyclic prefix and sub-carrier spacing. We also investigate algorithms for multi-user frequency estimation at the gateway.

The forward link timing synchronization is a simpler problem because all return channel via satellite terminals (RCSTs) receive transmission from the Network Control Center (NCC) and are therefore synchronized with the transmitter. Each RCST simply has to synchronize its receiver to the forward link frame and then extract its own information based on the allocated sub-carriers. However, in the return link, different users with different propagation delays transmit to the NCC on different sub-carriers within the same frame. In order to maintain orthogonality, it is essential that all RCSTs are time synchronized at the NCC. The SC-FDMA waveform depends strongly on frame timing and carrier frequency synchronization of all users in order to mitigate inter-symbol interference, inter-carrier interference, and multiple access interference (MAI).

Motivated by the aforementioned discussion, in this section, we discuss and propose solutions for synchronization acquisition and tracking. Synchronization acquisition focuses on frame timing offsets estimation at logon in order to correct differential propagation delays in the presence of residual frequency offsets and amplifier non-linearity. We assume that after synchronization acquisition, the magnitude of residual symbol timing and carrier frequency errors fall within the CP length and sub-carrier spacing, respectively. Therefore, synchronization tracking focuses on fractional frequency estimation for each user channel at the NCC.

5.1. Synchronization acquisition

Uplink synchronization in OFDMA systems has been extensively investigated in the past [18] for terrestrial systems, and some specific approaches have been implemented for the terrestrial long-term evolution (LTE) air interface [37–39]. The LTE approach is preamble based, and this is also compatible with the current DVB-RCS2 standard specifications [1]. Relatively, few papers have also studied various aspects of SC-FDMA synchronization for geostationary satellite channels [19, 20]. Timing alignment of the uplink transmissions in LTE is achieved by applying a timing advance at the user equipment (UE), relative to the received downlink timing [37–39]. The main role of this is to counteract differential propagation delays between UEs. After a UE has first synchronized to the downlink transmission, the initial timing advance is set by means of a random access procedure. This is then updated from time to time, to counteract changes in the arrival time of the uplink signals at the base station. Such changes may arise from the changes in propagation delay, oscillator drift in the UE, where the accumulation of small frequency errors over time may result in timing errors, and Doppler shift arising from the movement of the UE, thus resulting in an additional frequency offset of the uplink signals received at the base station.

It is assumed that each user acquires uplink synchronization at logon. Firstly, a user terminal acquires frame timing and carrier frequency parameters based on the forward link signal (e.g., second generation of DVB via satellite) at downlink synchronization. It is reasonable to assume that residual frequency errors, with regard to the downlink carrier in the forward link, are less than few multiples of the sub-carrier spacing, while residual timing errors with regard to the downlink frame are less than the CP duration.

In order to solve the problem of significantly larger propagation delays in the GEO satellite channel as compared with the terrestrial channel, we propose the use of global positioning system (GPS)-based timing pre-compensation at each RCST as shown in Figure 10.

This requires the implementation of a GPS device at each user terminal, which is considered affordable. The advantage of using this approach is that the RACH can be dimensioned with highly reduced overhead in terms of guard time. This is because a GPS device located at each RCST will track its current location with substantial accuracy. This can then be combined with the satellite location data and the NCC coordinates to calculate the specific propagation delay between the NCC and each RCST. The calculated delay can then be pre-compensated for each RCST before the random access procedure. The effect of using the proposed approach is that the timing misalignment (i.e., relative timing delay) between RCSTs is significantly reduced from an order of milliseconds to an order of nanoseconds as shown in Table I. The residual timing errors can easily be accommodated within an associated CP, as a negligible overhead.

For SC-FDMA synchronization acquisition in the satellite return link, a conventional approach such as in LTE is to dimension the RACH within an SC-FDMA superframe. The random access preambles used in the LTE standard are Zadoff–Chu (ZC) sequences, which have good periodic correlation

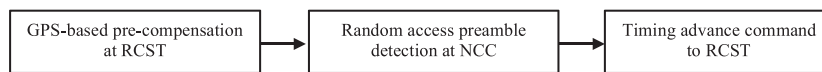


Figure 10. Uplink timing acquisition stages. RCST, return channel via satellite terminal; NCC, Network Control Center.

Table I. Pre-compensation accuracy.

Beam radius (A) (km)	600	300	100
Speed of light (C) (m/s)	$3 \cdot 10^8$		
Maximum two-way differential delay ($D = 2A/C$) (ms)	4	2	0.67
Minimum position accuracy of GPS device (E) (m)	10	10	10
Pre-compensation accuracy ($F = 2E/C$) (ns)	67	67	67

properties and robust performance in the presence of frequency offset [40–42]. Their constant amplitude property makes them an attractive option for non-linear transmissions [23] in the satellite return link. Therefore, the use of ZC sequences as training symbols can be combined with the use of CPM as data symbols, to achieve a robust SC-FDMA waveform in the satellite non-linear channel.

After downlink synchronization has been achieved in the forward link, the parameters of the RACH have been established, and GPS-based timing pre-compensation has been performed, each RCST transmits a random access preamble to the NCC based on ZC or pseudo-random noise sequences as shown in Figure 1. This is detected by the NCC as part of the uplink synchronization acquisition procedure (Figure 1) and the appropriate timing error established as integer multiples of the orthogonal frequency-division multiplexing (OFDM) sampling duration. The NCC then sends a timing advancement command to the RCST in order to pre-compensate for the detected timing errors. Furthermore, the integer frequency error within the RACH (if any) is established, and the terminal receives instruction to adjust its frequency accordingly. Each RCST must acquire synchronization at logon in order to maintain a synchronous SC-FDMA system.

5.2. Synchronization tracking

The satellite drift in GEO leads to differential Doppler shifts with respect to the different user terminals. As a baseline approach, it is proposed that the sub-carrier spacing of the SC-FDMA system is dimensioned to be greater than the maximum Doppler shift arising. This will guarantee that the carrier frequency offset (CFO) always has a fractional value at the tracking stage. This approach is necessary because the presence of significant MAI in the received signal at the NCC will degrade the frequency estimation accuracy.

In order to achieve reliable frequency synchronization, it is required to transmit training sequences within each user channel because the frequency offsets will vary per user transmission. We have investigated a viable approach for multi-user frequency estimation at the NCC based on sequences embedded within the shared user data channel. This includes a review of several frequency estimation algorithms for single-user OFDM systems [43–46] and how to adapt these algorithms to work in the multi-user SC-FDMA system. A general concept of frequency estimation as discussed in these algorithms is the use of repetitive symbols in the time domain. These can be appropriately designed in the frequency domain. A basic framework for achieving frequency synchronization tracking is shown in Figure 11. This corresponds to the uplink synchronization loop as shown in Figure 1. It includes transforming the received signal to the frequency domain in order to extract the received preamble sub-carriers for a specific user. These are then transformed back into the time domain with appropriate nulls assigned to the other user sub-carriers in order to obtain the time-domain equivalent signal with repetitive parts. Consequently, fractional frequency estimation and correction are both achieved in the time domain.

Figure 12 shows the estimation performance of a ZC-based preamble using Schmidl's method [44] for an SC-FDMA user transmission received in the gateway in the presence of inter-carrier interference, MAI, and Rapp non-linearity [23]. The preamble consists of a ZC sequence (root = 7 and length = 27) spread over a user channel of 64 sub-carriers per symbol in an SC-FDMA system with $N_{FFT} = 256$. A total of 10 sub-carriers are used as guard bands for the preamble in frequency domain, while the ZC sequence is transmitted as one SC-FDMA symbol with two identical parts. It can be seen that the algorithm achieves good performance close to the Cramer–Rao lower bound (CRLB) for frequency estimation in an AWGN channel for an observation window of N_{FFT} time-domain samples [18].

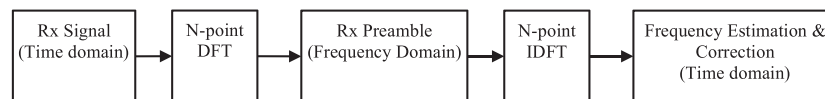


Figure 11. Uplink frequency tracking stages. DFT, discrete Fourier transform; IDFT, inverse discrete Fourier transform.

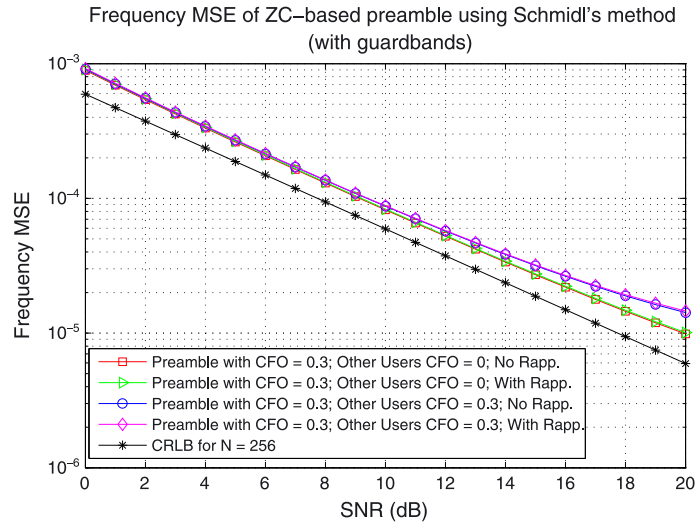


Figure 12. Frequency estimation performance (with guard bands). CFO, carrier frequency offset; CRLB, Cramer-Rao lower bound; MSE, mean square error; ZC, Zadoff-Chu.

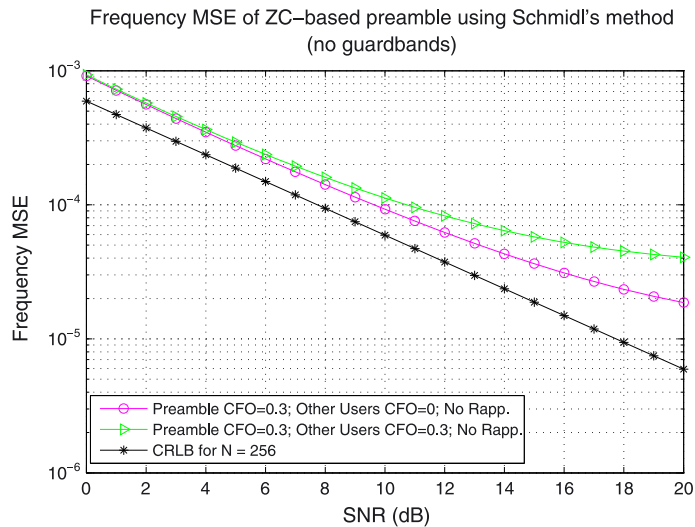


Figure 13. Frequency estimation performance (no guard bands). CFO, carrier frequency offset; CRLB, Cramer-Rao lower bound; MSE, mean square error; SNR, signal-to-noise ratio; ZC, Zadoff-Chu.

Figure 13 shows the estimation performance when no guard bands are used for the preamble. In this instance, the preamble consists of a ZC sequence (root = 7 and length = 32) spread over a user channel of 64 sub-carriers. It can be seen that the frequency mean square error degrades because of increased interference from adjacent users. Therefore, it is important to isolate the estimation bandwidth for robust estimation accuracy.

An important factor to note is that frequency estimation accuracy (as defined by the CRLB) increases with fast Fourier transform (FFT) size because there are more independent samples within the observation window. On the other hand, a large FFT size implies small sub-carrier spacing for a fixed carrier bandwidth, thereby resulting in a long OFDM symbol duration, which is consistent with a CP design for minimum overhead. Therefore, it can be said that the maximum Doppler shift arising due to the GEO satellite drift plays a critical role in the SC-FDMA system design, because it must be lower than the sub-carrier spacing.

6. CONCLUSIONS

Within the context of the DVB-RCS2 return link air-interface standard, in the research reported in this paper, we have worked towards the Tbit/s communication requirements as presented in the Advanced Research in Telecommunications Systems 1 program by ESA. More specifically, the focus of this paper has been on the lower layers by proposing an efficient mapping technique that exploits in a better way multi-carrier communications. Such type of communications has been selected because of its higher flexibility as compared with the more traditional single-carrier communications and because of the inherent advantage of considering a scheme already widely used in terrestrial communications.

The first set of results presented was a performance comparison between SC-FDMA waveforms, which employed classical QAM types LM and CPM using novel mapping schemes. For this, different types of power amplifier models have been used in order to assess the employed mapping techniques. It has been shown that the proposed CPM schemes are more robust to both in-band and out-of-band non-linear distortion. In addition, MER performance evaluation has shown that the use of CPM signal as opposed to the use of LM signals can lead to further improvements. It is noted that the use of multi-carrier systems for future broadband and broadcast satellite applications is very interesting and worth pursuing further. Indeed, the use of satellite multi-carrier communications, even coupled with CPM, would open many interoperability solutions between satellite and terrestrial state-of-the-art telecommunication systems in which multi-carrier communications are widely employed.

We have also investigated the performance of a MA-CPM scheme, termed as 2A-MSK. It was based upon the superposition of two MSK signals at the RF level and thus requires the use of an additional HPA. In comparing the performance of the proposed 2A-MSK scheme with other equivalent modulation schemes such as 16-QAM and 16-APSK as well as 2A-QPSK and two-amplitude OQPSK, various evaluation results have been obtained, including BER, TD, and SE. These results have been shown that, as compared with the 16-QAM types modulation schemes, the proposed scheme can significantly improve the SE in the presence of ACI. Specifically, the proposed 2A-MSK scheme can double the SE currently achieved by the CPM schemes proposed in the DVB-RCS2 standard. Although this can be achieved at the expense of increased power requirements by approximately 3 dB, it is underlined that increasing the SE is a major step forward towards achieving in the future Tbit/s capacities.

Finally, we have investigated a viable and efficient framework for achieving reliable timing and frequency synchronization in an SC-FDMA satellite return link. This involves a combination of GPS-based pre-compensation of differential timing between user terminals, preamble detection in an integrated RACH, and user channel frequency estimation based on repetitive symbols in the time domain. It has been shown that GPS-based delay pre-compensation can improve the frame timing uncertainty from an order of milliseconds to an order of nanoseconds, and this can be accommodated with the CP as a negligible overhead. Furthermore, the user channel frequency estimation is shown to be effective and close to the hard CRLB for the FFT size. The proposed synchronization technique would involve the implementation of a GPS receiver at each RCST. GPS receivers are commonly incorporated into many mobile devices nowadays. Hence, the additional cost incurred is considered negligible as compared with overall cost of the RCST.

ACKNOWLEDGEMENT

This work has been supported by the ESA in the framework of SATNEX III CoO3; 23089/10/NL/CLP.

REFERENCES

1. ETSI. Digital video broadcasting (DVB): second generation DVB interactive satellite system (DVB-RCS2) part 2: lower layers for satellite standard. *Technical Report EN 101 545-2 v1.1.1*, ETSI, 2012. (Available from: <http://www.etsi.org>).
2. ETSI. Digital video broadcasting (DVB); interaction channel for satellite distribution systems. *Technical Report EN 301 790 v1.3.1*, ETSI, 2003. (Available from: <http://www.etsi.org>).
3. ETSI. Digital video broadcasting (DVB); second generation DVB interactive satellite system (DVB-RCS2); part 1: overview and system level specification. *Technical Report TS 301 545-1 v1.1.1*, ETSI, 2012. (Available from: <http://www.etsi.org>).
4. ETSI. Digital video broadcasting (DVB); second generation DVB interactive satellite system (DVB-RCS2); part 2: lower layers for satellite standard. *Technical Report EN 301 545-2 v1.1.1*, ETSI, 2012. (Available from: <http://www.etsi.org>).

5. ETSI. Digital video broadcasting (DVB); second generation DVB interactive satellite system (DVB-RCS2); part 3: higher layers satellite specification. *Technical Report TS 301 545-3 v1.1.1*, ETSI, 2012. (Available from: <http://www.etsi.org>).
6. Kyrgiazos A, Evans B, Thompson P, Mathiopoulos PT, Papahalabos S. A terabit/second satellite system for European broadband access: a feasibility study. *International Journal of Satellite Communications and Networking* 2014; **32**(2): 63–92.
7. TERASAT - approaching the terabit/s satellite: a system study. (Available from: <https://artes.esa.int/projects/terasat-approaching-terabits-satellite-system-study>) [Accessed on 8 July 2015].
8. Perotti A, Tarable A, Benedetto S, Montorsi G. Capacity-achieving CPM schemes. *IEEE Transactions on Information Theory* 2010; **56**(4):1521–1541.
9. Beidas BF, Cioni S, De Bie U, Ginesi A, Iyer-Seshadri R, Kim P, Lee LN, Oh D, Noerpel A, Papaleo M, Vanelli-Coralli A. Continuous phase modulation for broadband satellite communications: design and trade-offs. *International Journal of Satellite Communications and Networking* 2013; **31**(5):249–262.
10. Colavolpe G, Montorsi G, Piemontese A. Spectral efficiency of linear and continuous phase modulations over nonlinear satellite channels. *Proceedings of 2012 IEEE International Conference on Communications (ICC)*, Ottawa, ON, Canada, 2012; 3175–3179.
11. Baroni R, Lombardo F, Suffritti R, Candreva EA, Vanelli-Coralli A, Corazza GE, Colavolpe G, Gallinaro G, Alagha N. Performance analysis of a mesh satellite system based on linear and continuous phase modulations. *Proceedings of 2012 IEEE International Conference on Communications (ICC)*, Ottawa, ON, USA, 2012; 3255–3259.
12. Kandus G, Lazic D, Senk V. Some characteristics of multi-amplitude CPM. *8th European Conference on Electrotechnics, 1988. Conference Proceedings on Area Communication, EUROCON 88*: Stockholm, 1988; 60–63.
13. Sahin A, Guvenc I, Arslan H. A survey on multicarrier communications: prototype filters, lattice structures, and implementation aspects. *IEEE Communications Surveys Tutorials* 2014; **16**(3):1312–1338.
14. Pun M, Morelli M, Kuo CCJ. *Multi-carrier Techniques for Broadband Wireless Communications*, World Scientific, 2007.
15. Tellado J. *Multicarrier Modulation with Low PAR: Applications to DSL and Wireless*, The Springer International Series in Engineering and Computer Science, Springer: Dordrecht, Netherlands, 2000.
16. Li H, Liu B, Liu H. Transmission schemes for multicarrier broadcast and unicast hybrid systems. *IEEE Transactions on Wireless Communications* 2008; **7**(11):4321–4330.
17. Weber IW, Stanton P, Sumida J. A bandwidth compressive modulation system using multi-amplitude minimum shift keying (MAMSK). *IEEE Transactions on Communications* 1978; **26**(5):543–551.
18. Morelli M, Kuo CC, Pun MO. Synchronization techniques for orthogonal frequency division multiple access (OFDMA): a tutorial review. *Proceedings of the IEEE* 2007; **95**(7):1394–1427.
19. Rossetto F, Berioli M. On synchronisation for SC-FDMA waveform over geo satellite networks. *2012 6th Advanced Satellite Multimedia Systems Conference (ASMS) and 12th Signal Processing for Space Communications Workshop (SPSC)*: Baiona, 2012; 233–237.
20. Wei L, Yongliang X, Haibo Y. The effect of satellite movement on two-way time synchronization performance. *2012 IEEE International Frequency Control Symposium (FCS)*: Baltimore, MD, 2012; 1–3.
21. ETSI. Digital video broadcasting (DVB): second generation framing structure, channel coding and modulation system for broadcasting, interactive services, news gathering and other broadband satellite applications. *Technical Report EN 302 307 v1.1.2*, 2006. (Available from: <http://www.etsi.org>).
22. Wylie-Green MP, Perrins E, Svenssons T. Introduction to CPM-SC-FDMA: a novel multiple-access power efficient transmission scheme. *IEEE Transactions on Communications* 2011; **59**(7):1904–1915.
23. Rapp C. Effects of HPA-nonlinearity on a 4-DPSK/OFDM-signal for a digital sound broadcasting signal. *Proceedings of ESA Second European Conference on Satellite Communications*, Liege, Belgium, 1991; 179–184.
24. Saleh AAM. Frequency-independent and frequency-dependent nonlinear models of TWT amplifiers. *IEEE Communications Magazine* 1981; **29**(11):1715–1720.
25. SATNEX. *Digital Satellite Communications*, Springer Verlag, 2007.
26. Sacchi C, Rossi T, Ruggieri M, Granelli F. Efficient waveform design for high-bit-rate w-band satellite transmissions. *IEEE Transactions on Aerospace and Electronic Systems* 2011; **47**(2):974–995.
27. Dalakas V, Mathiopoulos PT, Di Cecca F, Gallinaro G. A comparative study between SC-FDMA and OFDMA schemes for satellite uplinks. *IEEE Transactions on Broadcasting* 2012; **58**(3):370–378.
28. Piazza R, Shankar B, Zenteno E, Rönnow D, Grotz J, Zimmer F, Grasslin M, Heckmann F, Cioni S. Multicarrier digital pre-distortion/equalization techniques for non-linear satellite channels. *Proceedings of 30th AIAA International Communications and Satellite Systems Conference (ICSSC)*, Ottawa, ON, Canada, 2012; 1–5.
29. Chuberre N, Courseille O, Laine P, Rouillet L, Quignon T, Tatar M. Hybrid satellite and terrestrial infrastructure for mobile broadcast services delivery: an outlook to the unlimited mobile TV system performance. *International Journal of Satellite Communications and Networking* 2008; **26**(5):405–426.
30. Next generation broadcasting system to handheld, physical layer specification (DVB-NGH), 2012. *BlueBook A160*, DVB.
31. Second generation DVB interactive satellite system (DVB-RCS2); part 4: guidelines for implementation and use of EN 301 545-2. *Technical Report 101 545-4*, ETSI, 2014.
32. Candreva EA, Tarchi D, Vanelli-Coralli A, Corazza GE. Robust SC-FDMA subcarrier mapping for non-linear channels. *2014 7th Advanced Satellite Multimedia Systems Conference and the 13th Signal Processing for Space Communications Workshop (ASMS/SPSC)*, Livorno, Italy, 2014; 360–365.
33. Digital video broadcasting (DVB); measurement guidelines for DVB systems. *Technical Report 101 290*, ETSI, 2014.

34. Kandus G, Lazic D, Senk V. Transmitter and receiver structures for multi-amplitude CPM. *Electrotechnical Conference, 1989. Proceedings. 'Integrating Research, Industry and Education in Energy and Communication Engineering', MELECON '89, Mediterranean, 1989*; 433–435, 437.
35. Binh LN. Multi-amplitude minimum shift keying modulation format for optical communications. *Optics Communications* 2008; **281**:4245–4253. provided by the SAO/NASA Astrophysics Data System.
36. SatNEx. CoO3Task 1 final report: capacity enhancement techniques for multibeam satellite networks. *Technical Report ESA Contract 23089/10/NL/CLP*, DLR, 2014.
37. Sesia S, Toufik I, Baker M. *LTE, The UMTS Long Term Evolution: From Theory to Practice*, Wiley InterScience Online Books, Wiley, 2009.
38. 3GPP, 3rd generation partnership project. Technical specification group radio access network; evolved universal terrestrial radio access (E-UTRA); physical channels and modulation (Release 11). *Technical Report TS 36.211*, 2013. (Available from: <http://www.etsi.org>).
39. 3GPP, 3rd generation partnership project. Technical specification group radio access network; evolved universal terrestrial radio access (E-UTRA); physical layer procedures (Release 11). *Technical Report TS 36.213*, 2013. (Available from: <http://www.etsi.org>).
40. Chu D. Polyphase codes with good periodic correlation properties (corresp.). *IEEE Transactions on Information Theory* 1972; **18**(4):531–532.
41. Wen Y, Huang W, Zhang Z. Cazac sequence and its application in LTE random access. *IEEE Information Theory Workshop, 2006. ITW '06*, Chengdu, 2006; 544–547.
42. Kim S, Joo K, Lim Y. A delay-robust random access preamble detection algorithm for LTE system. *2012 IEEE Radio and Wireless Symposium (RWS)*; Santa Clara, CA, 2012; 75–78.
43. Moose PH. A technique for orthogonal frequency division multiplexing frequency offset correction. *IEEE Transactions on Communications* 1994; **42**(10):2908–2914.
44. Schmidl T, Cox D. Robust frequency and timing synchronization for OFDM. *IEEE Transactions on Communications* 1997; **45**(12):1613–1621.
45. Morelli M, Mengali U. An improved frequency offset estimator for OFDM applications. *Communication Theory Mini-conference*; Vancouver, BC, 1999; 106–109.
46. Awoseyila A, Kasparis C, Evans B. Robust time-domain timing and frequency synchronization for OFDM systems. *IEEE Transactions on Consumer Electronics* 2009; **55**(2):391–399.

AUTHORS' BIOGRAPHIES



P. T. Mathiopoulos (SM' 1994) received his PhD degree in digital communications from the University of Ottawa, Canada, in 1989. From 1982 to 1986, he was with Raytheon Canada Ltd., working in the areas of air navigational and satellite communications. In 1988, he joined the Department of Electrical and Computer Engineering (ECE), University of British Columbia (UBC), Canada, where he was a faculty member until 2003, holding the rank of Professor from 2000 to 2003. From 2000 to 2014, he was with the Institute for Space Applications and Remote Sensing (ISARS), National Observatory of Athens (NOA), first as its Director and then as Director of Research, where he established the Wireless Communications Research Group. As ISARS' Director (2000–2004), he has led the Institute to a significant expansion R&D growth, and international scientific recognition. For these achievements, ISARS has been selected as a national Centre of Excellence for the years 2005 to 2008. Since 2014, he is an Adjunct Researcher at the Institute of Astronomy, Astrophysics, Space Applications, and Remote Sensing (IAASARS) of NOA. Since 2003, he also taught part-time at the Department of Informatics and Telecommunications, University of Athens, where he is Professor of Digital Communications since 2014. From 2008 to 2013, he was appointed as Guest Professor at the Southwest Jiaotong University, China. He has been also appointed by the Government of China as a Senior Foreign Expert at the School of Information Engineering, Yangzhou University (2014–2015) and by Keio University, Japan, as a Visiting Professor in the Department of Information and Computer Science (2015).

For the last 25 years, he has been conducting research mainly on the physical layer of digital communication systems for terrestrial and satellite applications, including digital communications over fading and interference environments. He co-authored a paper in GLOBECOM'89 establishing for the first time in the open technical literature the link between MLSE and multiple (or multi-symbol) differential detection for the AWGN and fading channels. He is also interested in channel characterization and measurements, modulation and coding techniques, synchronization, SIMO/MIMO, UWB, OFDM, software/cognitive radios, and green communications. In addition, since 2010, he has been actively involved with research activities in the fields of remote sensing, LiDAR systems, and photogrammetry. In these areas, he has co-authored more than 100 journal papers, mainly published in various IEEE and IET journals, four book chapters and more than 120 conference papers. He has been PI for more than 40 research grants and has supervised the thesis of 11 PhD and 23 Master students.

Dr. Mathiopoulos has been or currently serves on the editorial board of several archival journals, including the IET Communications, and the IEEE Transactions on Communications (1993–2005). He has regularly acted as a

consultant for various governmental and private organizations. Since 1993, he has served on a regular basis as a scientific advisor and a technical expert for the European Commission (EC). In addition, since 2001, he has served as the Greek representative to high-level committees in the EC and the European Space Agency (ESA). He has been a member of the TPC of more than 70 international IEEE conferences and the TPC Vice Chair for the 2006-S IEEE VTC and 2008-F IEEE VTC, as well as Co-Chair of FITCE2011. He has delivered numerous invited presentations, including plenary lectures, and has taught many short courses all over the world. As a faculty member at the ECE of UBC, he was elected ASI Fellow and a Killam Research Fellow. He is a co-recipient of two best paper awards for papers published in the 2nd International Symposium on Communication, Control, and Signal Processing (2008) and 3rd International Conference on Advances in Satellite and Space Communications (2011).



E. A. Candreva was born in Venice (Italy) in 1983. He studied at the Collegio Superiore of the University of Bologna, receiving his BS and MS degrees (summa cum laude) and Ph.D in Telecommunication Engineering from the University of Bologna in 2004, 2006, and 2010, respectively. He worked as a senior staff engineer in the ICT Solutions department at Mavigex, Bologna, and as a post-doctoral research engineer at the University of Bologna. Currently, he is an automotive electronics consultant at AKKA Italia. Dr. Candreva is co-recipient of the Best Student Paper Award at ICSSC 2009 and has co-authored more than 20 scientific publication and served as invited speaker and lecturer.



A. B. Awoseyila received the BSc Hons. degree in Electronics and Electrical Engineering from the Obafemi Awolowo University (O.A.U), Ile-Ife, Nigeria in 1998. He also received MSc. and PhD degrees in Mobile and Satellite Communications from the University of Surrey, U.K. in 2005 and 2008, respectively. Since then, he has been with the Institute for Communication Systems (ICS), University of Surrey, UK in research and teaching of satellite communications with a main focus on air interface. He is currently a senior researcher at ICS, and his research expertise covers signal processing techniques for wireless communications and physical/link layer techniques for satellite-mobile communications. He has held a patent in OFDM synchronization and has published some well-cited papers in IEEE and IET journals.



V. Dalakas obtained a BSc in Physics, an MSc degree (honors) in digital signal processing, and a PhD degree in digital communications, all from the University of Athens (UoA), Greece, in 1998, 2002, and 2010, respectively. Since 2001, he has been affiliated with the Harokopio University of Athens (HUA), Greece, as a Research Fellow (since 2001) and as a network and system administrator since 2005. His research interests include wireless digital communications and modeling and simulation standardization methods. In these areas, he has co-authored several papers and two book chapters.



D. Tarchi(S'99, M'05, SM'12) received an MSc degree in Telecommunications Engineering and a PhD degree in Informatics and Telecommunications Engineering from the University of Florence, Italy, in 2000 and 2004, respectively. From 2004 to 2010, he has been a research fellow and then a research associate at the University of Firenze, Italy. Since 2010, he has been an assistant professor at the University of Bologna, Italy. His research interests are in both data link and physical layers, with particular interests on resource allocation algorithms in wireless networks. He has not only been involved in several national projects as well as European projects and has also been active in several industry-funded projects. He is an editorial board member for the Hindawi Journal of Engineering and Hindawi, the Scientific World Journal since 2012 and has served as an associate editor for IEEE Transactions on Wireless Communications from 2008 to 2013. He has been a symposium chair at IEEE WCNC 2011 and at IEEE Globecom 2014, a workshop co-chair at the IEEE ICC 2015, and a publicity chair for a workshop within IWCMC'09, IWCMC'10, and IWCMC'11. He is an IEEE Senior Member since February 2012.



B. G. Evans has BSC and PhD degrees from the University of Leeds, is a Fellow of the UK Royal Academy of Engineering and the IET and senior member of IEEE and AIAA. From 1968 to 1983, he was British Telecom lecturer to Reader at the University of Essex in Telecommunication systems. He was appointed to the Alec Harley Reeves chair of Information systems engineering at the University of Surrey in 1983 and was founder Director of the Centre for satellite engineering research and then the Centre for Communication Systems Research. He was Dean of Engineering from 1999 to 2001 and Pro-Vice Chancellor for research and Enterprise from 2001 to 2009.

Barry Evans has researched in satellite communications, radio propagation, signal processing and networking and has over 600 publications in the literature plus three books. He is Editor of the International Journal of Satellite communications.



A. Vanelli-Coralli (S'93, M'97, SM'07) is an Associate Professor and chairperson of the PhD Board on Electronics and Telecommunications at the University of Bologna. He has been Project Coordinator of the FP7 project CoRaSat (Cognitive Radio for Sat-Com), and Scientific Responsible for several European Space Agency and European Commission-funded projects.



G. E. Corazza PhD, is a Full Professor in Telecommunications at the Alma Mater Studiorum University of Bologna, the oldest academic institution of the Western world. Since 2012, he has been a Member of the University of Bologna Board of Directors, the highest governance body in the institution. He was Head of the Department of Electronics, Computer Science and Systems (DEIS) in the years 2009–2012 and Chairman of the School for Telecommunications in the years 2000–2003. He is not only the President of the Scientific Council of the Fondazione Guglielmo Marconi but is also a Member of the Marconi Society Board of Directors. Giovanni E. Corazza is the founder of the Marconi Institute for Creativity, a body created as a joint initiative of the Fondazione Guglielmo Marconi and the University of Bologna, to investigate and divulgate all of the most research scientific evidence on the creative thinking process in humans and in artificially intelligent machines.

Since 2014, he is a Vice-Chairman of NetWorld2020, the European Technology Platform dedicated to the future evolution of communication networks, and Member of the Board of the 5G Infrastructure Association, the private side of the 5G-PPP with the European Commission. Moreover, Corazza was the Chairman of the Advanced Satellite Mobile Systems Task Force (ASMS?TF) and Founder and Chairman of the Integral Satcom Initiative (ISI), a European Technology Platform devoted to Satellite Communications. He was a co-founder of Mavigex S.r.l., a spin-off company dedicated to the development of innovative smartphone applications. During his career, he also worked for Qualcomm (California, USA) and COM DEV (Ontario, Canada). He has been the principal investigator in more than 20 European projects funded by the European Commission and by the European Space Agency. He is a Member of the Editorial Board of the Journal of Eminence and Genius. In the years 1997–2012, he has served as Editor for Communication Theory and Spread Spectrum for the IEEE Transactions on Communications. He is author of two books and of more than 300 papers on diversified topics in wireless and satellite communications, mobile radio channel characterization, Internet of things, navigation and positioning, estimation and synchronization, spread spectrum and multi-carrier transmission, scientific creative thinking. Furthermore, Corazza received the Marconi International Fellowship Young Scientist Award in 1995, the IEEE 2009 Satellite Communications Distinguished Service Award, the 2013 Newcom# Best Paper Award, the 2002 IEEE VTS Best System Paper Award, the Best Paper Award at IEEE ISSSTA'98, at IEEE ICT2001, and at ISWCS 2005. He has been the General Chairman of the IEEE ISSSTA 2008, ASMS 2004–2012 Conferences, and the MIC Conference 2013. He has taught several graduate and undergraduate courses on digital transmission, mobile radio communications, principles of multimedia applications and services, software for telecommunications, information theory and coding, digital receiver design and optimization, creativity and innovation. He is a Member of the Scientific Committee of the Bologna Business School, where he contributes also to the Executive Master in Technology and Innovation Management.